

Figure S1

A

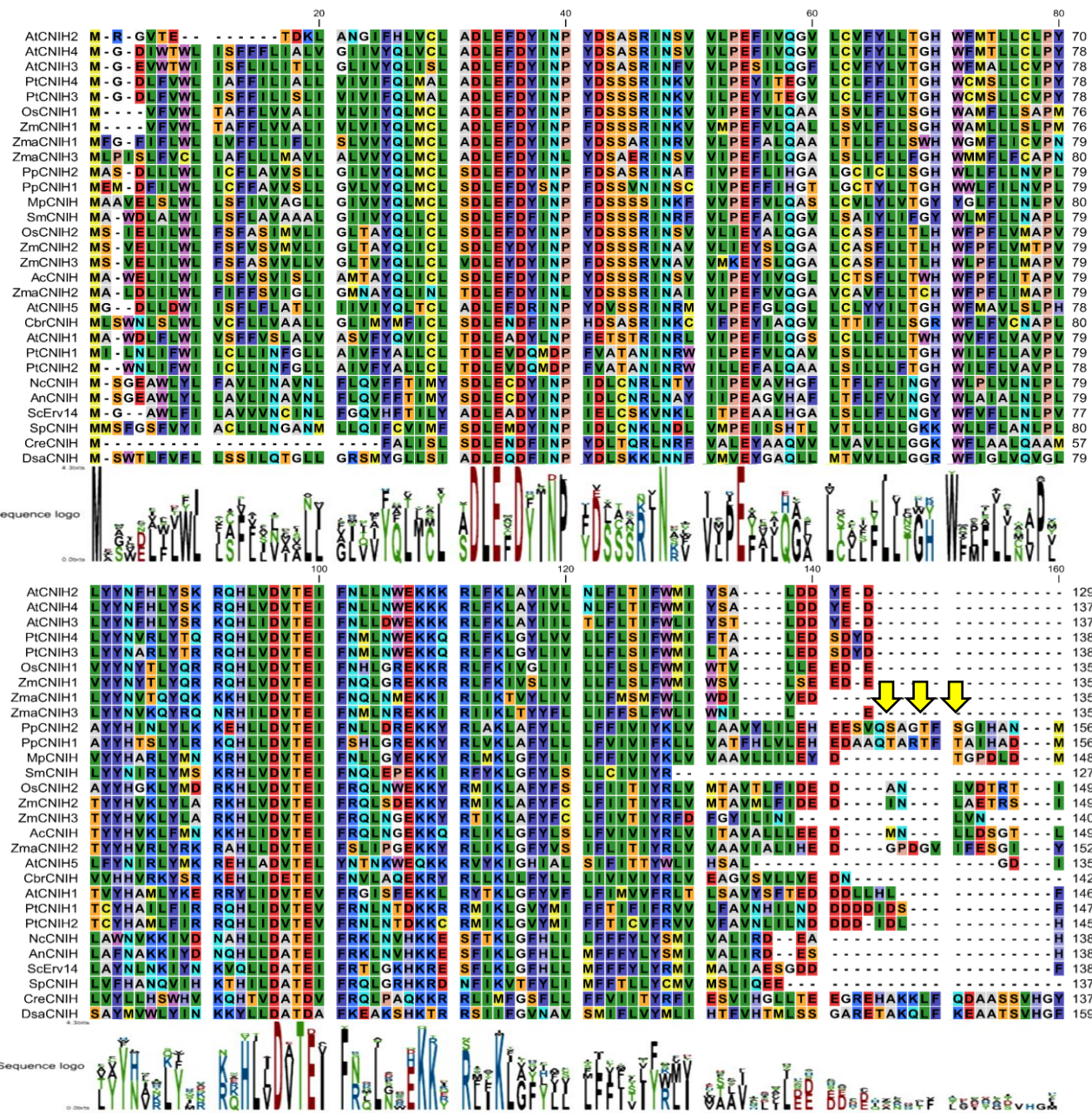


Fig. S1. Multiple amino acid sequence alignment of cornichon homolog proteins and putative phosphorylation sites in moss homologs. Amino acid sequence alignment of cornichon homologs from algae, plants, and fungi; solid and dashed bars show the consensus motif IFNXL, the acidic motif (Ac. Dom), respectively. Arrows indicate predicted phosphorylation sites on Ser and/or Thr residues identified by the NetPhos3.1 prediction server.

Figure S2

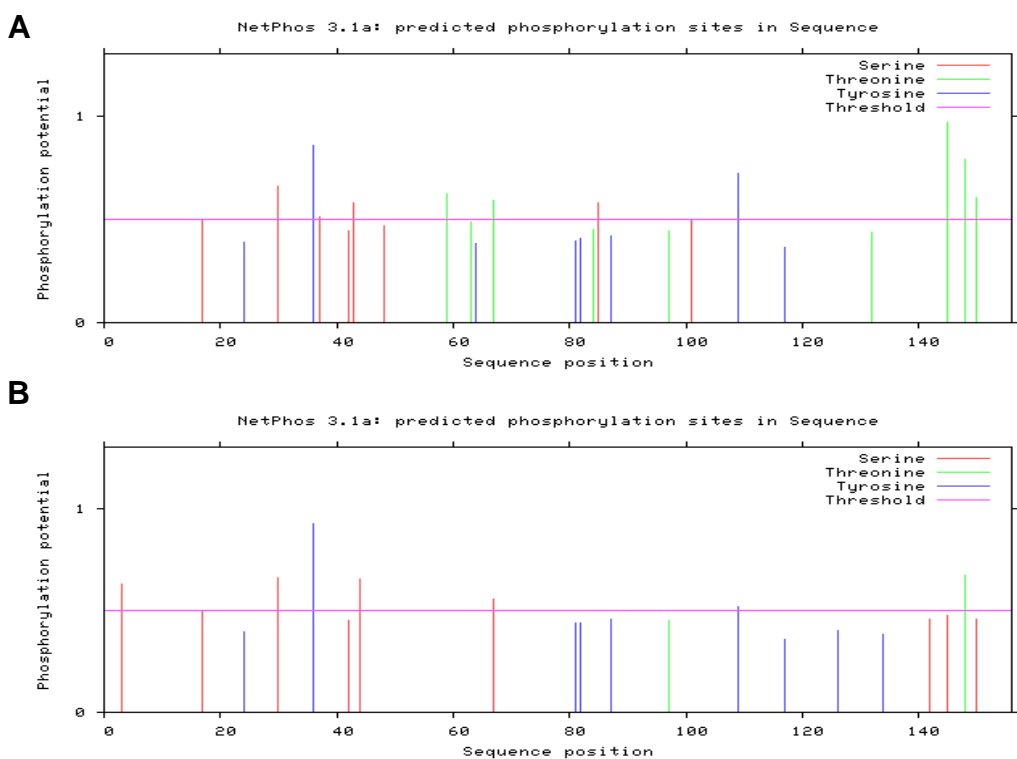


Fig. S2. In silico analysis of putative phosphorylation sites of moss cornichon proteins and proteins pairwise comparison matrix. Predicted phosphorylation sites for CNIH1 A) and CNIH2 B) proteins. Serine, Threonine and Tyrosine are shown in red, green and blue, respectively; in silico analysis was performed with the NetPhos3.1 server (https://services.healthtech.dtu.dk/service.php?NetPhos-3.1).

Figure S3

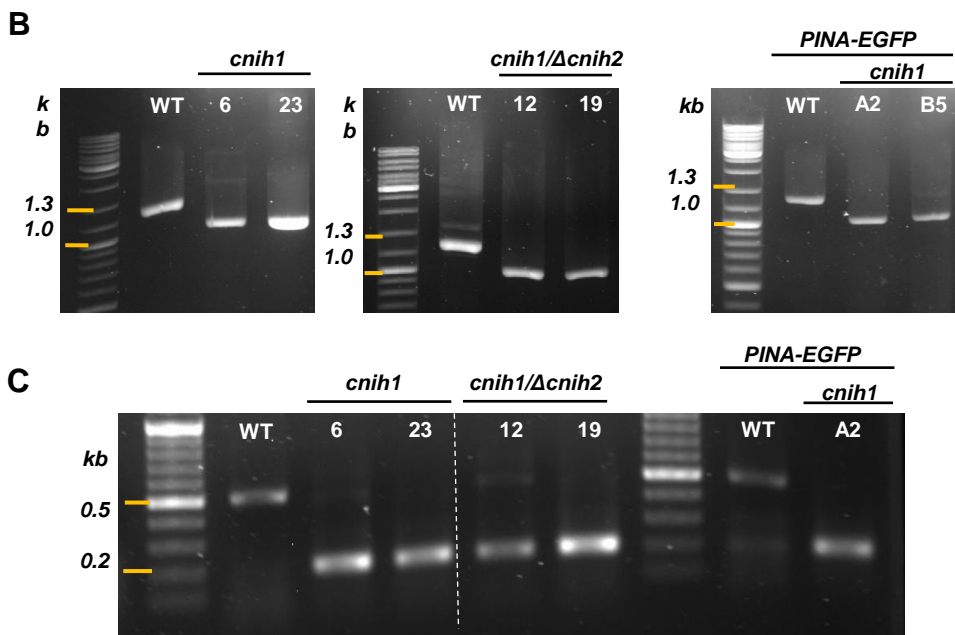
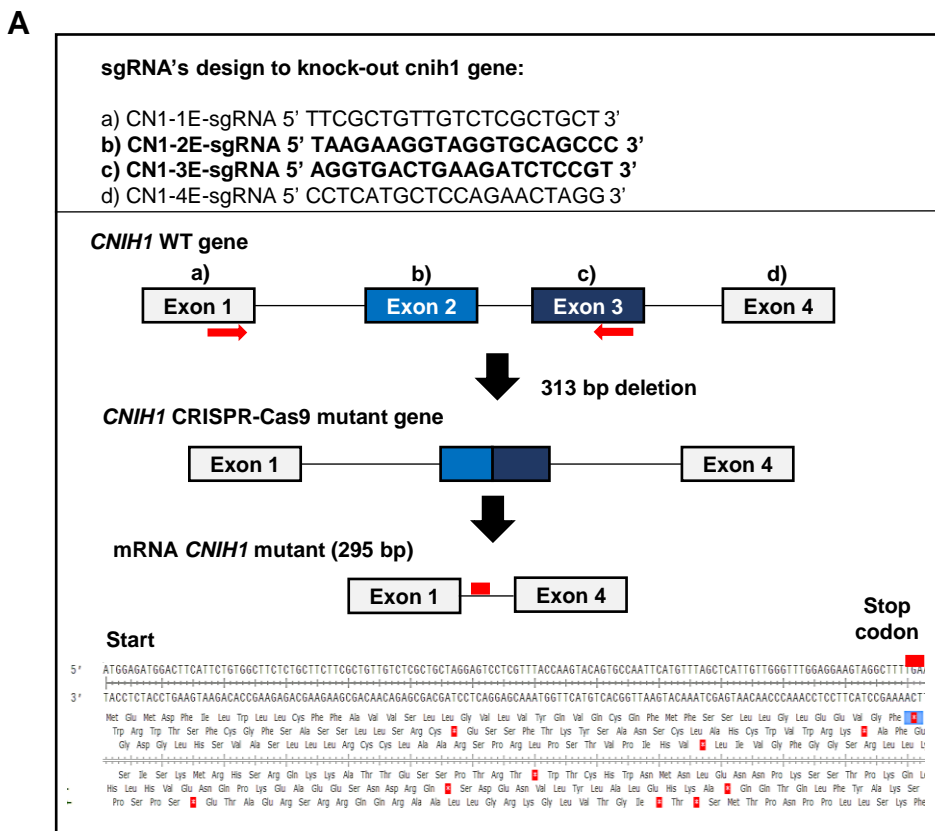


Fig. S3. Generation of *cnih1* mutant lines by the CRISPR-Cas9 system. A)

Schematic strategy for mutation of the *CNIH1* gene by the CRISPR-Cas9 system. Four different sgRNA were synthesized (a to d); each sgRNA targeted one of the four exons of the *CNIH1* gene. Only the b and c sgRNA's (bold type) were efficient and deleted a total of 313 bp (removing the second intron and part of Exon 2 and Exon 3) resulting in the *cnih1* mutant line. This mutation generated an in-frame premature stop codon at nucleotide 132 (indicated by a red line) that codifies for 43 amino acids (predicted peptide size of 5 kDa). **B)** Comparison of the PCR products from the WT *CNIH1* gene (1,309 bp); the single *cnih1* mutant lines (1,000 bp) (#6 and #23) and double *cnih1/Δcnih2* mutant lines (#12, #19) in WT parental line, and in the reporter PINA-EGFP lines (A2, B5). Amplified PCR bands from genomic DNA extractions. **C)** Comparison between WT *CNIH1* and *cnih1* single mutant coding sequences (cDNA). Agarose DNA gel (1%) shows amplified PCR bands from cDNA of WT *CNIH1* (468 bp); *cnih1* single mutant lines (295 bp) (#6 and #23) and double *cnih1/Δcnih2* mutant lines (#12 and #19), and in the *cnih1* PINA-EGFP single mutant line (A2).

Figure S4

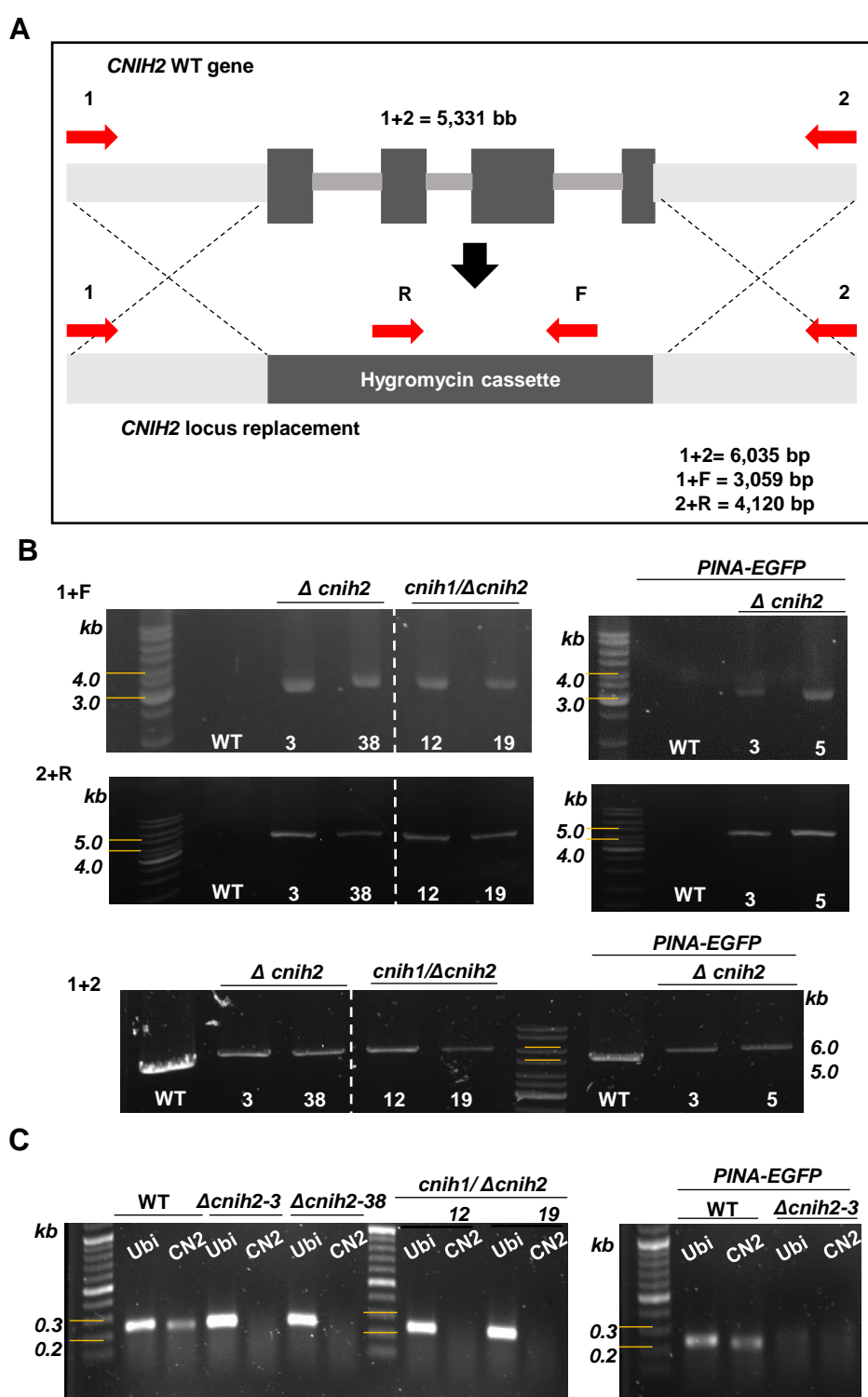


Fig. S4. Generation of $\Delta cnih2$ mutant lines and their genotypification. **A)** *CNIH2* disruption strategy showing the genomic location of *CNIH2* locus and primers (red arrows) for genetic analyses. **B)** Agarose DNA gel (1%) showing the presence and the replacement by the hygromycin cassette by PCR amplified products from WT and $\Delta cnih2$ single mutant lines (#3 and #38), *cnih1*/ $\Delta cnih2$ double mutants (#12 and #19), and $\Delta cnih2$ single mutant lines (#3 and #5) in the PINA-EGFP genetic line. **C)** Agarose DNA gel (1%) shows amplified PCR bands from cDNA of *CNIH2* (468 bp) in WT and in PINA-GFP lines, in comparison with the absence of *CNIH2* mRNA transcript in the $\Delta cnih2$ single mutant lines (#3 and #38), *cnih1*/ $\Delta cnih2$ double mutant lines (#12 and #19) and $\Delta cnih2$ /PINA-GFP line (#3).

Figure S5

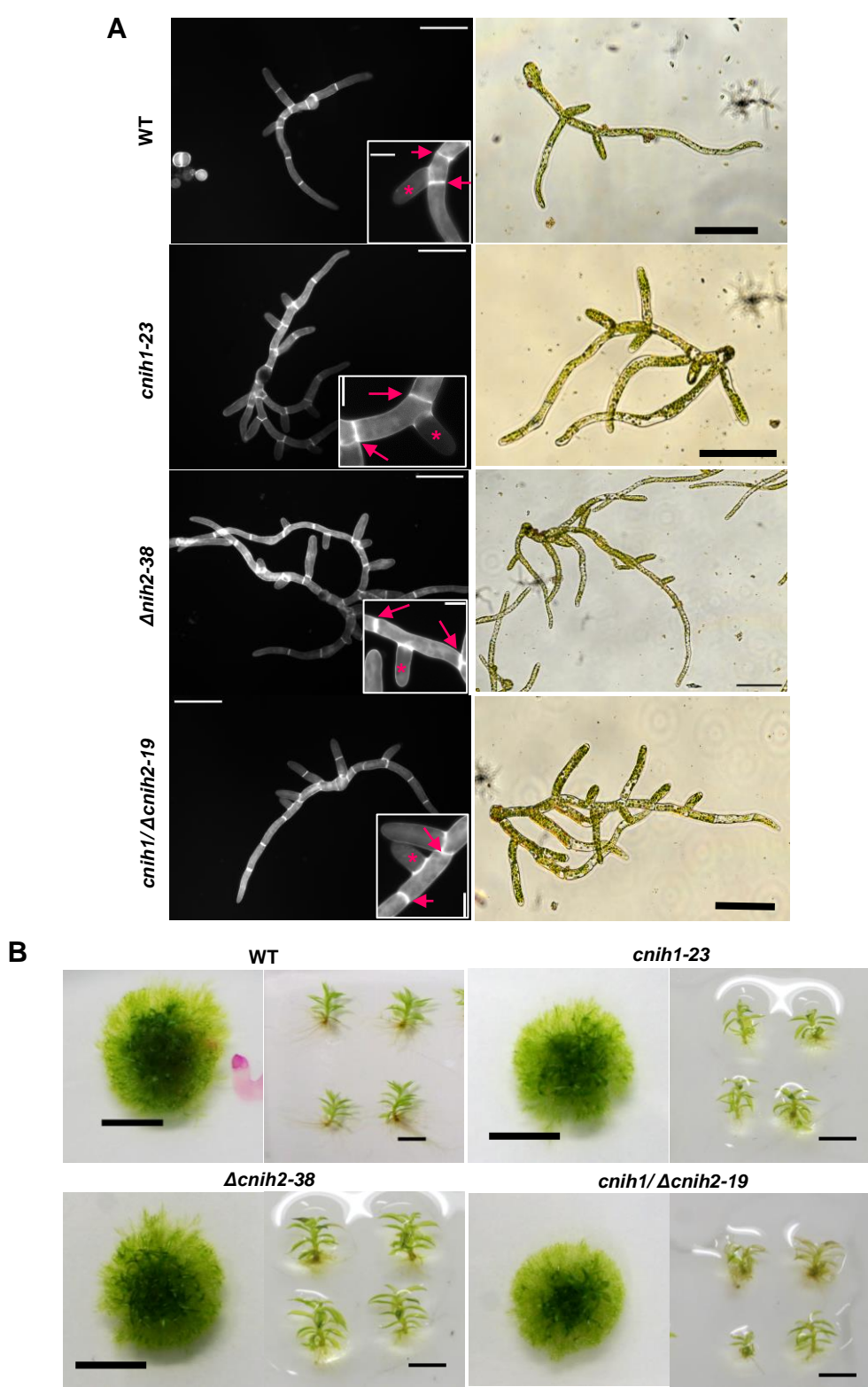


Fig. S5. Cornichon mutants have pleiotropic effects during the moss life cycle. **A)** (Left panel) Protonema from WT and cornichon mutants stained with Calcofluor White after 7 d growth, visualized in an epifluorescence microscope; scale = 100 µm. Insets shows cell divisions (arrows) and lateral initial branch cell (*). (Right panel) Brightfield images of seven-day-old protonema from WT and cornichon mutants, Scale 100 µm. **B)** Colony (top, scale 5 mm) and individual gametophores (bottom, scale 2 mm) from WT and cornichon mutants after four weeks of growth.

Figure S6

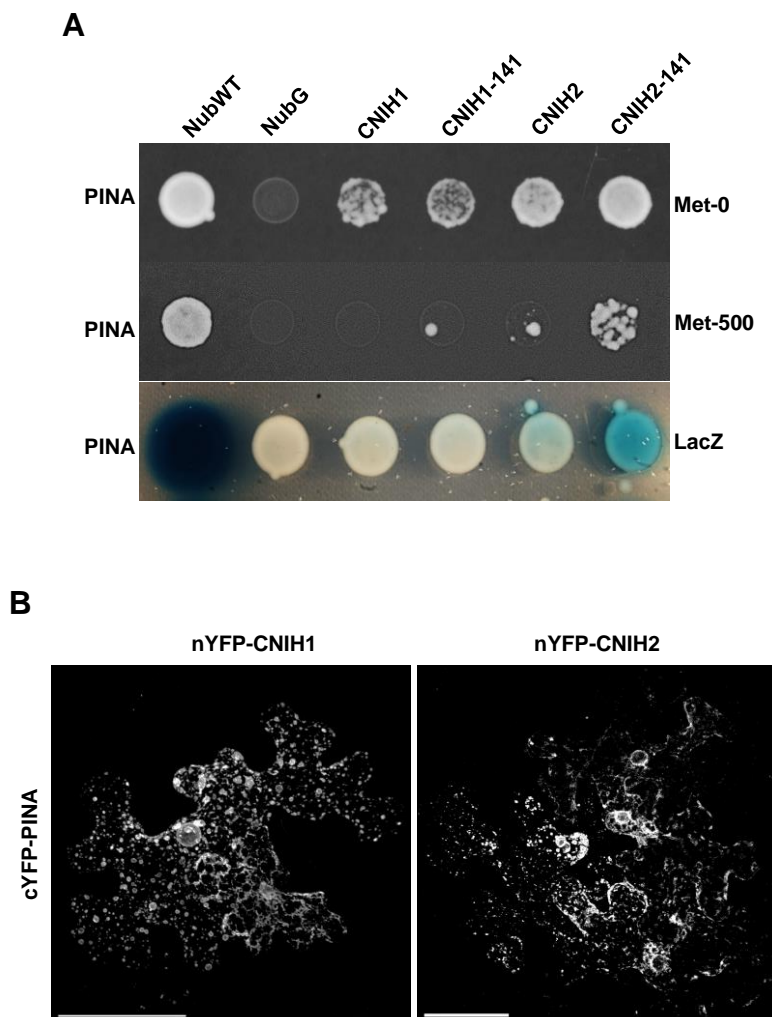
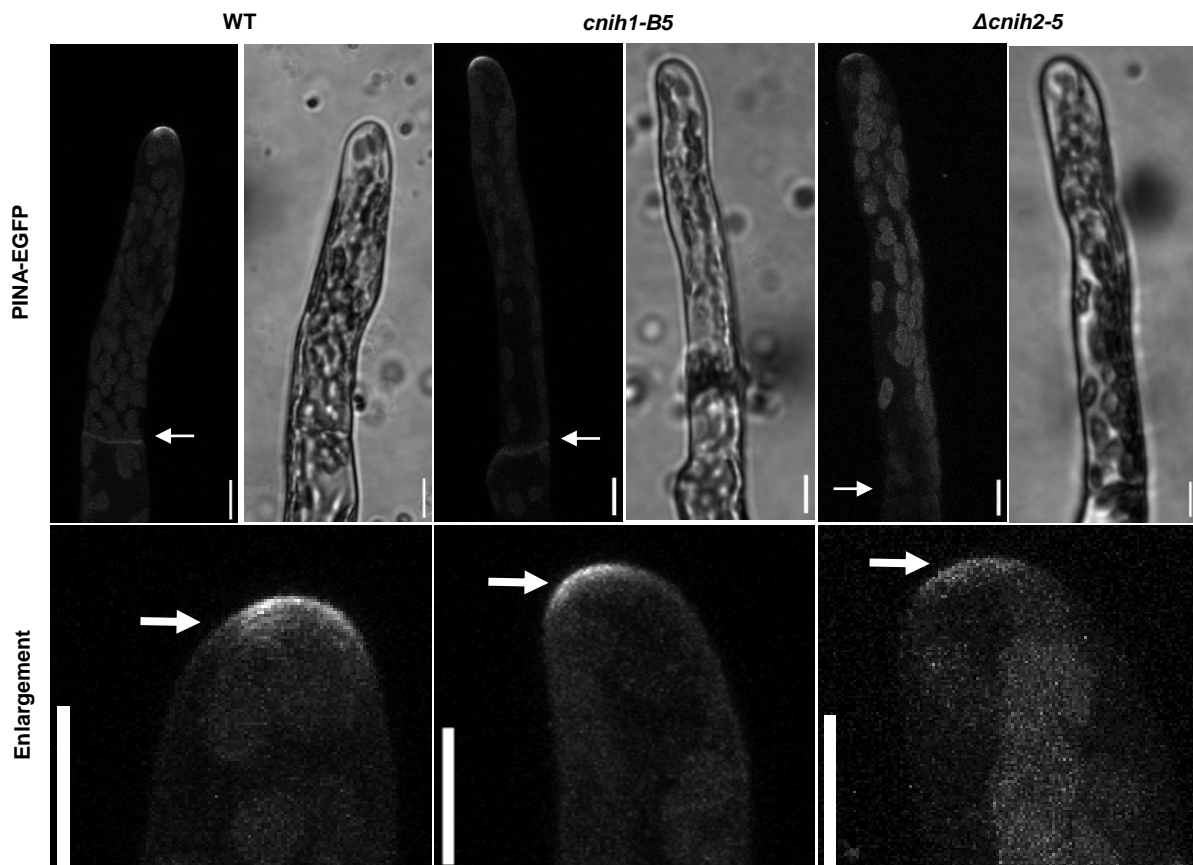


Fig. S6. CNIH2 protein is the cargo receptor for the auxin transporter PINA.

A) Protein-protein interaction identified by the mbSUS assay with the moss cornichon WT, CNIH1-141 and CNIH2-141 proteins (Nub fusions) and the auxin transporter PINA (Cub fusion). Yeast cell growth in selection medium (Met-0); the strength of the interaction was confirmed by cell growth inhibition under repressive selection conditions (Met-500) and by the lower activity of LacZ (intensity of the bluish color). NubWT and NubG were used as false negative and false positive controls, respectively. **B)** Original images of Figure 3B, showing interaction between PINA and CNIH1 or CNIH2 was confirmed by reconstitution of split-YFP fluorescence by the co-expression of nYFP-CNIH's with c-YFP-PINA proteins, scale = 50 μ m.

Figure S7

A



B

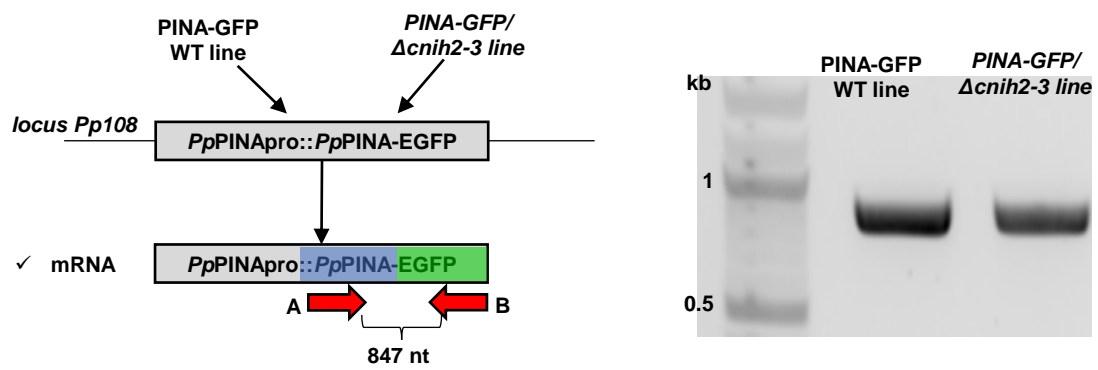


Fig. S7. Subcellular localization of the auxin efflux transporter PINA in additional *cnih1* and *Δcnih2* single mutants. **A)** (top) Localization of PINA in WT and cornichon single mutants in a protonema apical cell. Fluorescence at the tip and the base (arrow) was maintained in the *cnih1-B5* single mutant, but not in the *Δcnih2-5* single mutant. (bottom) ROI enlargement of PINA-EGFP fluorescence at the tip of the apical protonema cells from WT, *cnih1-B5*, and *Δcnih2-5* mutant lines. Scale = 10 μ m. **B)** (left) Schematic representation of the *PpPINAPro::PpPINAPINAE GFP* construct inserted at the locus *Pp108* in WT (PINA-EGFP) and *Δcnih2-3* single mutant line; primers A and B were used to amplify a 847 nt corresponding 130 nt of PINA coding sequence (primer A) and 717 nt of the EGFP coding sequence (primer B) in the PINA-EGFP reporter line parental/background; (right) 1% agarose DNA gel showing expected PCR products confirming the presence of the PINA-EGFP transcript in both, over-expressing and *Δcnih2-3* mutant lines.

Figure S8

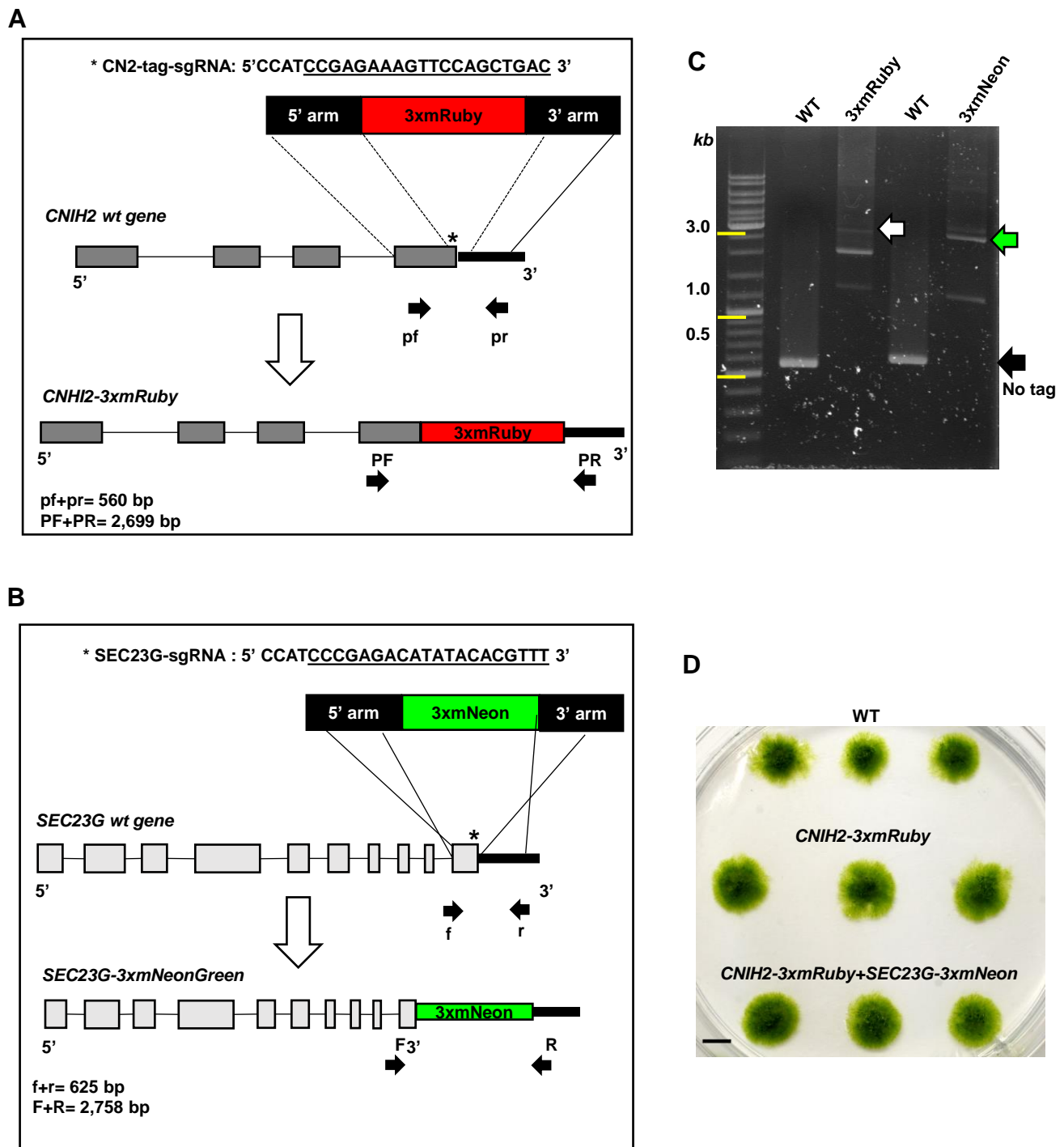


Fig. S8. Generation of CNIH2-3xmRuby and SEC23G-3xmNeon Knock-in lines by CRISPR-Cas9 & HDR. **A)** Design and representation of CNIH2-3xmRuby stable line at the C-terminus of the gene. sgRNA sequence guide for making a double break in DNA (asterisk) and 3xmRuby coding sequence flanked by recombination homolog sequences. Primers pf and pr amplified a fragment of 557 bp by PCR in WT line without inserting the tag. Primers PF and PR amplified a fragment of 2,699 bp by PCR in WT line with the insertion of a 3xmRuby tag. **B)** Design and representation of SEC23G-3xmNeon stable line at the C-terminus of the gene. sgRNA sequence guide for making a double break in DNA (asterisk) and 3xmNeon coding sequence flanked by recombination homolog sequences. Primers f and r amplified a fragment of 625 bp by PCR in the WT line without inserting the tag. Primers F and R amplified a fragment of 2,758 bp by PCR in WT line with the insertion of a 3xmNeon tag. **C)** 1% agarose DNA gel showing expected PCR products in the knock-in CNIH2-3xmRuby line (white arrow), SEC23G-3xmNeon line (green arrow), and without any tag (black arrow). **D)** Moss colonies from CNIH2-3mxRuby and CNIH2-3xmRuby+SEC23G-3xmNeon lines grown together with the WT line. Scale= 2 mm.

Figure S9

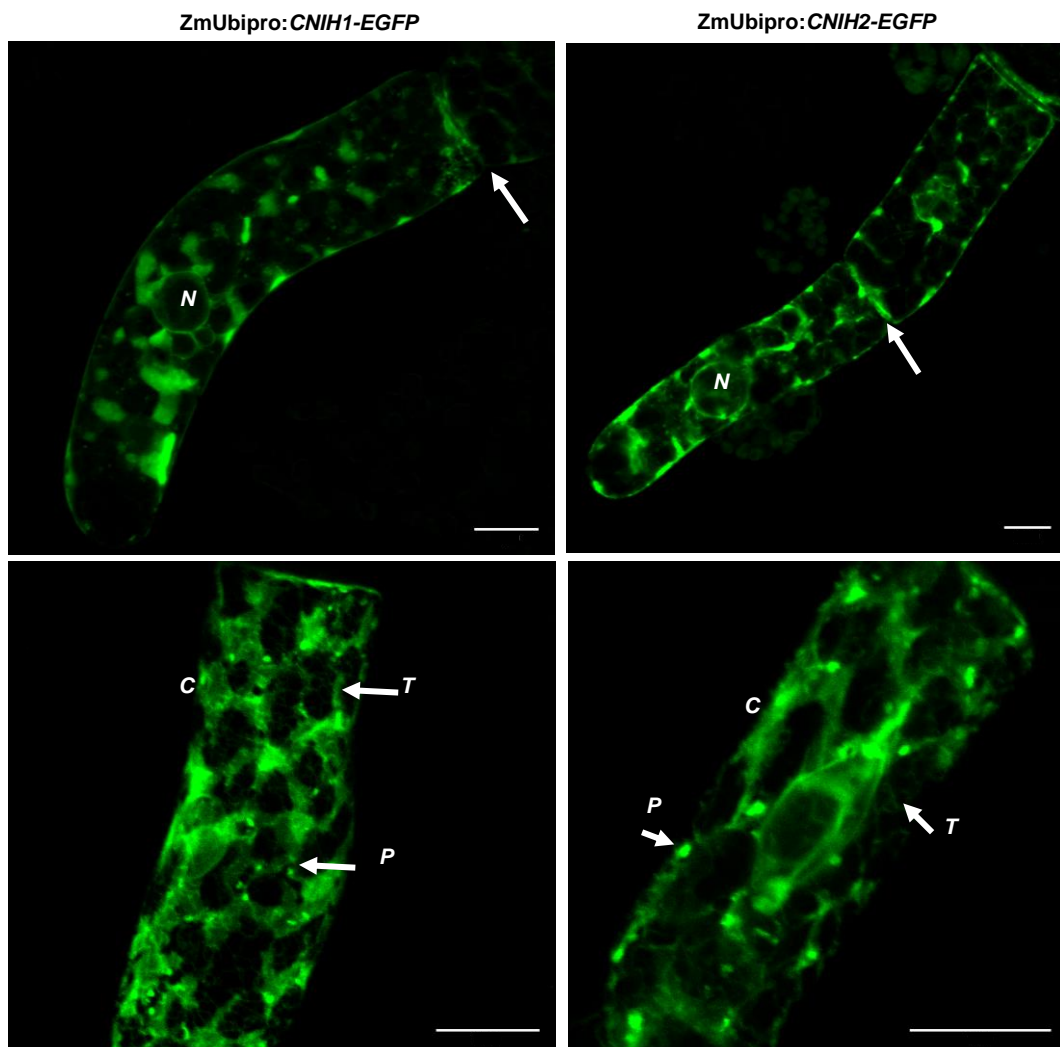


Fig. S9. Overexpression of moss cornichon proteins localized mainly at ER but also in puncta. Confocal images showing the subcellular localization of transiently expressed *ZmUbipro::CNIH1-EGFP* (left column) and *ZmUbipro:CNIH2-EGFP* (right column) from seven-day-old apical protonemal cells. Arrows indicate localization of the cell plate for both proteins (top row). N = nucleus. Identification of moss cornichons at ER subdomains as tubules (T) and cisternae (C), and in puncta below ER (P) (bottom row), scale 10 μ m.

Figure S10

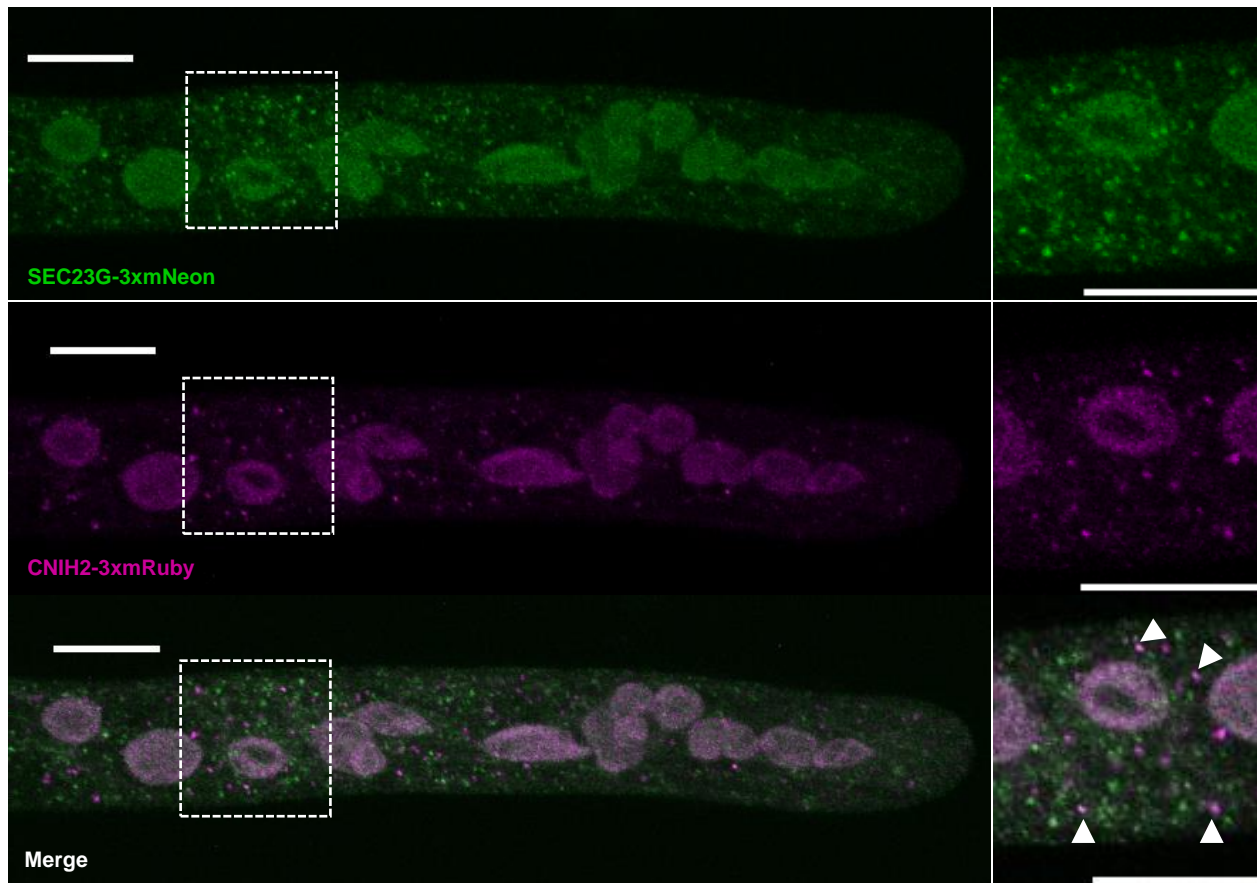
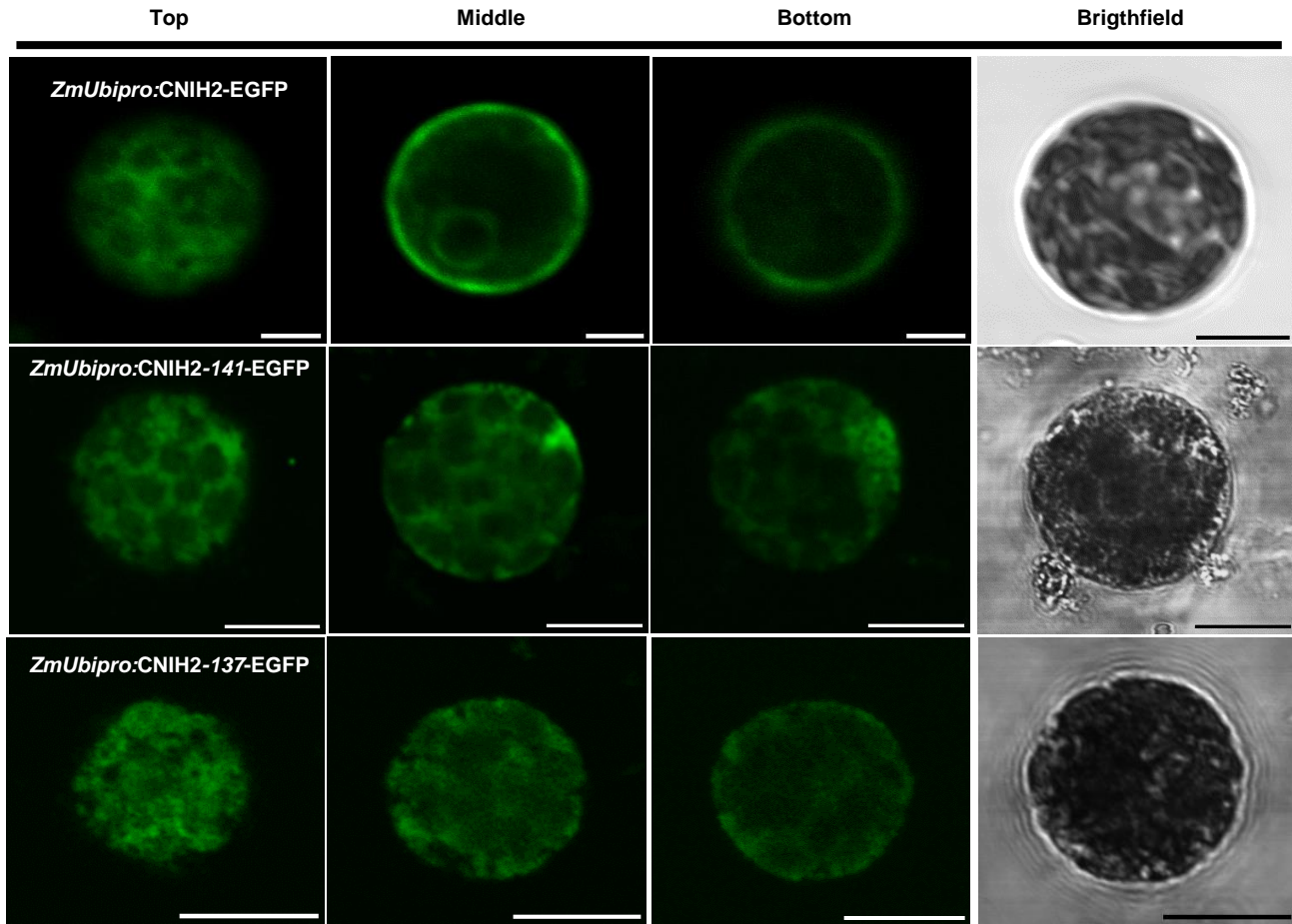


Fig. S10. Co-localization of CNIH2 and SEC23G. Original images of endogenous SEC23G (top panel), CNIH2 (middle panel) and merge images (bottom panel) of endogenous CNIH2 and SEC23G tagged proteins in a protonemal apical cell; (right) enlargement of the region delimited (dashed squares). Representative Z-projection with maximal intensity confocal image; scale 10 μ m.

Figure S11

A



B

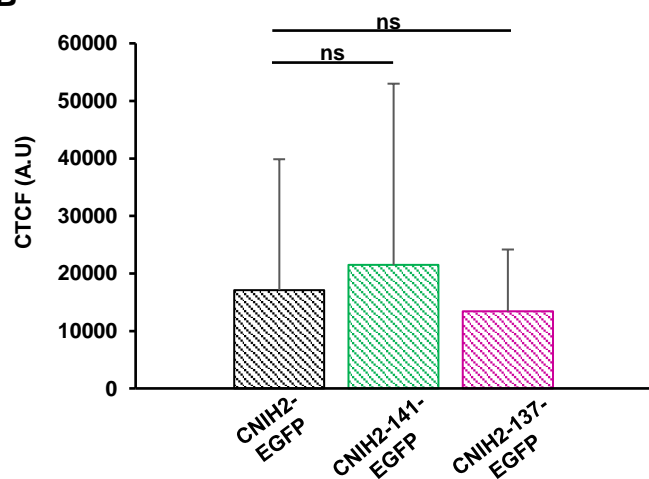


Fig. S11. Expression of WT CNIH2 and C-terminal truncated proteins in WT moss protoplasts. **A)** Confocal images showing localization of transiently overexpressed WT *ZmUbipro::CNIH2-EGFP* (top row) and C-terminus truncated protein versions *ZmUbipro::CNIH2-141-EGFP* (middle row) and *ZmUbipro::CNIH2-137-EGFP* (bottom row) in moss protoplasts at 48 h after transformation, showing a reticulate subcellular localization. Images from three individual optical sections (Top, Middle and Bottom) of the protoplasts. Scale 10 μ m. **B)** Fluorescence intensity of moss protoplasts transformed with the WT and CNIH2 C-terminus truncated fusion constructs. CTFC = corrected total cell fluorescence. n = 4; data are the mean \pm SD t-test was performed for statistics (ns p \geq 0.05).

Table S1. Primers list

Name	SEQUENCE 5' – 3' Cloning	References
attB1 (5' half sequence)	GGGGACAAGTTGTACAAAAAAGCAGGCT	This study
attB2 (5' half sequence)	GGGGACCACTTGTACAAGAAAGCTGGGT	This study
PpCNIH1-For	GTACAAAAAAGCAGGCTTCATGGAGATGGACTTC	This study
PpCNIH1-Rev	GTACAAGAAAGCTGGTCCATGTCTCGCTGGATTG	This study
PpCNIH2-For	GTACAAAAAAGCAGGCTTCATGGCTCCGATCTCC	This study
PpCNIH2-Rev	GTACAAGAAAGCTGGTCCATGGCTGGATC	This study
PpCNIH2-141-Rev	GTACAAGAAAGCTGGTCTTCATGCTCAAGAAATTAAAG	This study
PpCNIH2-137-Rev	GTACAAGAAAGCTGGTCAAGAAATTAAAGTAGACGGCTGC	This study
PpCNIH1 disruption by CRISPR-Cas9 system		
sgRNACN1-1E-null-Rv	AAACAGCAGCGAGACAACAGCGAA	
sgRNACN1-1E-null-Fwd	CCATTCGCTGTTGTCGCTGCT	
sgRNACN1-2E-Fwd	CCATTAAGAAGGTAGGGCGAGCCC	This study
sgRNACN1-2E-Rv	AAACGGGCTGCACCTACCTTCTTA	This study
sgRNACN1-3E-Fwd	CCATACGGAGATCTCAGTCACCT	This study
sgRNACN1-3E-Rv	AAACAGGTGACTGAAGATCTCCGT	This study
sgRNACN1-4E-Fwd	CCATCCTCATGCTCCAGAACTAGG	This study
sgRNACN1-4E-Rv	AAAC CCTAGTTCTGGAGCATGAGG	This study
Genotyping PpCNIH1 CRISPR-Cas9 mutants		
CN1-null-Fwd	CCATTCGCTGTTGTCGCTGCT	This study
D-cni1-KO-Rv	GGACGTATGGACTGAATCC	This study
PpCNIH2 Knock-out disruption by Homologous recombination		
ATTB1-CNI2-M-Fw	GGGGACAAGTTGTACAAAAAAGCAGGCTGGGTTAACGATAGTGAGAGTGAGATGATTG AGG	This study
ATTB4-CNI2-M-Rv	GGGGACAACTTGTATAAGAAAGTTGGTGGCTCCCGGCTTCGCTGCTCCTCTC	This study
ATTB3-CNI2-4R-Fw	GGGGACAACTTGTATAAAAGTTGAATTCTCTTGGTCTGAGCCCATTGG	This study
ATTB2-CNI2-4R-Rv	GGGGACCACTTGTACAAGAAAGCTGGTAGTTAACAAATTCTCGCTGAACTAC	This study
Genotyping PpCNIH2 knock-outs		
Higro-F	GTCTGTCGAGAACGTTCTGATCG	
Higro-R	CGTCGGTTCCACTATCGG	
CN2-outer-up-F	GGAACGTACATGAGATGTGTCAAG	This study
CN2-outer-DW-R	CTCCCTCGTGTACTCCTCC	This study
C2-F	GCTGTTCTGCTCAACGTTCC	This study
C2-R	CTGACTGGACAGATTCTCATGC	This study
Ubi10-F	ACTACCTCGAAGTTGTATAGTTGG	
Ubi10-R	CAAGTCACATTACTCGCTGTCTAG	
PpCNIH2 Knock-in generation by CRISPR-Cas9&HDR		
CN2-tag-Fwd	CCATCCGAGAACGTTCCAGCTGAC	This study
CN2-tag-Rv	AAACGTCACTGGAACCTTCAGG	This study
pENT-CN2-Up-mut-Fw	GAATCTGTaCAGTCAGCTGGAAC	This study
pENT-CN2-Up-mut-Rv	GCTGACTGTACAGATTCTC	This study
B1-CNIH2-tag-Fwd	GGGGACAAGTTGTACAAAAAAGCAGGCTCGTCTTGCCTACATCACACG	This study
B4-CNIH2-tag-Rv	GGGGACAACTTGTATAAGAAAGTTGGTGCATGTTGCGTGGATCCCCGAGAAAG	This study
B3-CNIH2-tag-Fwd	GGGGACAACTTGTATAAAAGTTGCCTTGTGACTGTACACTGAACC	This study
B2-CNIH2-tag-Rv	GGGGACCACCTTGACAAGAAAGCTGGTAGCAAGACATGAGCTAGATACCAAC	This study
PpCNIH2-3xmRuby line screening		
cn2-downarm-Fwd	CATGTATCGTTCTGTCATG	This study
cn2-uparm-Rv	GATGTCATGTCAATACCAATG	This study
PpSEC23G-3xmNeon line screening		
S23g-int-F	GCTACTGATCAATGTTGACTGG	This study
S23g-int-R	GAACTAGTTCACTACTCCACG	This study
Transcript expression of PpPINa-EGFP knock-in line		
EGFP-Fwd	TAAACGCCACAAGTTCAGCG	This study
pinA-Rv	GAGAGGTGCCACCTATTGCAACC	This study